



UvA-DARE (Digital Academic Repository)

Dynamical structure factor of the anisotropic Heisenberg chain in a transverse field

Caux, J.S.; Essler, F.H.L.; Löw, U.

Published in:
Physical Review B

[Link to publication](#)

Citation for published version (APA):

Caux, J. S., Essler, F. H. L., & Löw, U. (2003). Dynamical structure factor of the anisotropic Heisenberg chain in a transverse field. *Physical Review B*, 68, 134431.

General rights

It is not permitted to download or to forward/distribute the text or part of it without the consent of the author(s) and/or copyright holder(s), other than for strictly personal, individual use, unless the work is under an open content license (like Creative Commons).

Disclaimer/Complaints regulations

If you believe that digital publication of certain material infringes any of your rights or (privacy) interests, please let the Library know, stating your reasons. In case of a legitimate complaint, the Library will make the material inaccessible and/or remove it from the website. Please Ask the Library: <http://uba.uva.nl/en/contact>, or a letter to: Library of the University of Amsterdam, Secretariat, Singel 425, 1012 WP Amsterdam, The Netherlands. You will be contacted as soon as possible.

Dynamical structure factor of the anisotropic Heisenberg chain in a transverse field

Jean-Sébastien Caux,¹ Fabian H. L. Essler,² and Ute Löw³

¹*ITFA, U. of Amsterdam, Valckenierstraat 65, 1018 XE Amsterdam, The Netherlands*

²*Department of Physics, Brookhaven National Laboratory, Upton, New York 11973-5000, USA*

³*Institut für Theoretische Physik, Universität zu Köln, Zùlpicher Strasse 77, 50937 Köln, Germany*

(Received 11 April 2003; published 20 October 2003)

We consider the anisotropic Heisenberg spin-1/2 chain in a transverse magnetic field at zero temperature. We first determine all components of the dynamical structure factor by combining exact results with a mean-field approximation recently proposed by Dmitriev *et al.* [JETP **95**, 538 (2002)]. We then turn to the small anisotropy limit, in which we use field theory methods to obtain exact results. We discuss the relevance of our results to neutron scattering experiments on the one-dimensional Heisenberg chain compound Cs₂CoCl₄.

DOI: 10.1103/PhysRevB.68.134431

PACS number(s): 75.10.Jm

I. INTRODUCTION

The spin- $\frac{1}{2}$ Heisenberg chain is one of the most well-understood paradigms for quantum critical behavior. The latter term is coined to describe a situation in which quantum fluctuations induce a critical behavior as a parameter such as doping or a magnetic field is varied. There are many physical realizations of models of (weakly coupled) Heisenberg chains in anisotropic antiferromagnets. Whereas these materials usually display a magnetic long-range order at very low temperatures $T < T_N$, which is induced by the weak coupling between chains, there is a large “window” above T_N where quantum fluctuations dominate and a scaling associated with a quantum critical disordered ground state is observed.¹ An obvious question concerns the fate of the intriguing physical properties such as the absence of coherent magnon excitations associated with the “Heisenberg quantum critical point,” if a magnetic field is applied or “XY”-like exchange anisotropies are present. It has been known for a long time that critical behavior persists in both cases and there is an entire quantum critical manifold rather than just a point. In this regime a host of exact results on thermodynamic quantities as well as dynamical correlation functions is available (see, e.g., Ref. 2 and references therein). On the other hand, if one combines an exchange anisotropy with a magnetic field that is at an angle to the anisotropy axis, altogether different physics emerges.³ The transverse field breaks the continuous U(1) symmetry of rotations around the anisotropy axis and the ground state develops a long-range Néel order. Another interesting feature is that the transversality of the field prevents the uniform magnetization from reaching saturation except for infinitely strong fields.

The main motivation for our work are recent neutron scattering experiments on the quasi-one-dimensional antiferromagnet Cs₂CoCl₄ (Ref. 4) in the presence of a magnetic field. It was suggested in Ref. 4 that an appropriate starting point for a description of these experiments is the anisotropic spin-1/2 Heisenberg chain in a transverse magnetic field

$$\mathcal{H} = J \sum_j S_j^x S_{j+1}^x + \Delta S_j^y S_{j+1}^y + S_j^z S_{j+1}^z + H S_j^z, \quad (1)$$

with $\Delta \approx 0.25$. In view of our interest in Cs₂CoCl₄, we will often consider $\Delta = 0.25$ in what follows, but our results are more general. The inelastic neutron scattering intensity is proportional to

$$I(\omega, \mathbf{k}) \propto \sum_{\alpha, \beta} \left(\delta_{\alpha\beta} - \frac{k_\alpha k_\beta}{\mathbf{k}^2} \right) S^{\alpha\beta}(\omega, \mathbf{k}), \quad (2)$$

where $\alpha, \beta = x, y, z$ and the dynamical structure factor $S^{\alpha\beta}$ is defined by

$$S^{\alpha\beta}(\omega, \mathbf{k}) = \frac{1}{2\pi N} \sum_{j,l=1}^N \int_{-\infty}^{\infty} dt e^{-ik \cdot \mathbf{R}_l + i\omega t} \langle S_j^\alpha(t) S_{j-l}^\beta(0) \rangle_c. \quad (3)$$

Here the subindex denotes the connected part of the correlator. For a three-dimensional system of uncoupled one-dimensional chains we have $\mathbf{R}_l = l a_0 \mathbf{e}$, where \mathbf{e} is a unit vector pointing along the chain direction. The dynamical structure factor then depends only on the component of the momentum transfer along \mathbf{e} , which we will denote by k .

The outline of this paper is as follows: In Sec. II we summarize essential steps of the mean-field approximation of Dmitriev *et al.* We then discuss the region of applied fields in which we believe the mean-field approximation to be applicable. In Sec. III we use exact methods to determine all nonzero components of the dynamical structure factor within the framework of the mean-field approximation. In Sec. IV we derive exact results for the structure factor in the small anisotropy limit by employing field theory methods. In Sec. V we discuss a field theory approach to the weak field limit. Section VI contains a discussion of our results in the context of the neutron scattering experiments on Cs₂CoCl₄.

II. MEAN-FIELD APPROXIMATION

Let us first review the main ingredients of the mean-field approximation (MFA) proposed by Dmitriev *et al.* in Ref. 5. We note that the MFA can be applied to the XYZ chain in a magnetic field as well. One first performs a Jordan-Wigner transformation, which yields the spinless fermion Hamiltonian

$$\mathcal{H}_0 = \sum_j \frac{J_+}{2} (c_j^\dagger c_{j+1} + \text{H.c.}) + \frac{J_-}{2} (c_j^\dagger c_{j+1}^\dagger + \text{H.c.}) + (n_j - 1/2)(n_{j+1} - 1/2) + H(n_j - 1/2). \quad (4)$$

Here the hopping and pairing matrix elements are $J_\pm = (1 \pm \Delta)/2$ and we have put $J = 1$. The pairing term is a consequence of the anisotropy of the model: it vanishes at the isotropic point $\Delta = 1$. In the MFA the four-fermion interaction term is decoupled in all possible ways. The relevant expectation values for the on-site magnetization, pairing, and kinetic term are denoted by

$$\mathcal{M} = \langle n_j \rangle - 1/2, \quad P = \langle c_{j+1} c_j \rangle, \quad K = \langle c_{j+1}^\dagger c_j \rangle. \quad (5)$$

The mean-field Hamiltonian is then

$$\mathcal{H}_{\text{MF}} = \sum_j \frac{\tilde{J}_+}{2} c_j^\dagger c_{j+1} + \frac{\tilde{J}_-}{2} c_j^\dagger c_{j+1}^\dagger + \text{H.c.} + \tilde{H} \sum_j (n_j - 1/2), \quad (6)$$

where we have dropped an unimportant constant, and defined the (real) parameters

$$\tilde{J}_+ = J_+ - 2K, \quad \tilde{J}_- = J_- + 2P, \quad \tilde{H} = H + 2\mathcal{M}. \quad (7)$$

The theory is now purely quadratic in fermion operators, and can thus be solved exactly. An alternative picture of this theory is obtained by Jordan-Wigner transforming back to spin variables, yielding an anisotropic xy model in a field,

$$\frac{\mathcal{H}_{xy}}{\tilde{J}_+} = \sum_j [(1 + \gamma) S_j^x S_{j+1}^x + (1 - \gamma) S_j^y S_{j+1}^y + h S_j^z] \quad (8)$$

with $\gamma = \tilde{J}_- / \tilde{J}_+$ and $h = \tilde{H} / \tilde{J}_+$. This model has been extensively studied in the literature and many useful results on correlation functions are available.^{6–10} For our purposes, we first need to complete the mean-field setup above by providing the necessary self-consistency conditions. First, we use the fact that the free fermionic theory can be Fourier transformed and diagonalized using a Bogoliubov-de Gennes (BdG) transformation, which reads, explicitly,

$$\begin{aligned} c_k &= \alpha_+(k) c'_k + i \alpha_-(k) c'_{-k}, \\ c'_{-k} &= -i \alpha_-(k) c'_k + \alpha_+(k) c'_{-k} \end{aligned} \quad (9)$$

with parameters

$$\alpha_\pm(k) = \frac{1}{\sqrt{2}} \left[1 \pm \frac{\tilde{J}_+ \cos k + \tilde{H}}{\omega(k)} \right]^{1/2}. \quad (10)$$

In the thermodynamic limit, the Hamiltonian becomes

$$\frac{\mathcal{H}_{\text{MF}}}{N} = \int_0^\pi \frac{dk}{2\pi} \mathbf{c}'^\dagger(k) \begin{pmatrix} \omega_+(k) & 0 \\ 0 & \omega_-(k) \end{pmatrix} \mathbf{c}'(k), \quad (11)$$

in which the Nambu spinors have bands $\omega_\pm(k) = \pm \omega(k)$,

$$\omega(k) = \tilde{J}_+ \sqrt{(\cos k + h)^2 + \gamma^2 \sin^2 k}. \quad (12)$$

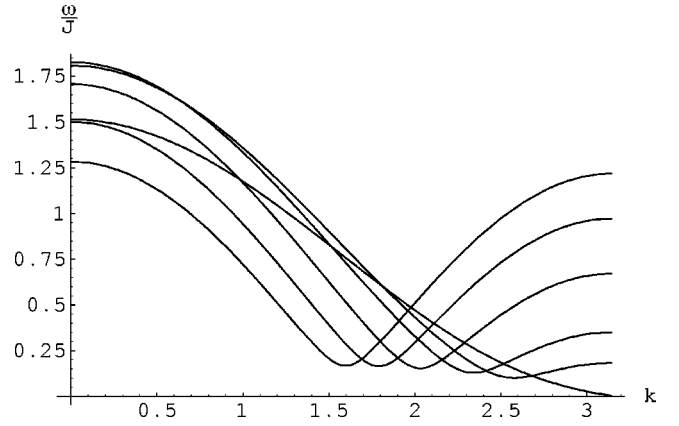


FIG. 1. Dispersion relation for $\Delta=0.25$ and external magnetic fields $H=0.05, 0.2, 0.4, 0.8, 1.2,$ and 1.6 (top to bottom at $k = \pi$).

This dispersion relation is plotted in Fig. 1 for $\Delta=0.25$ and various values of the external field. For $\Delta=0.25$ the gap vanishes for a critical field of $H_c = 1.604$ (corresponding to $h=1$). The self-consistency conditions at $T=0$ can be cast in the form

$$\mathcal{M}_i = \int_0^\pi \frac{dk}{2\pi} \frac{\partial \omega_-(k)}{\partial \tilde{H}_i}, \quad (13)$$

where we have defined the shorthand notations $\mathcal{M}_0 = \mathcal{M}, \mathcal{M}_1 = K, \mathcal{M}_2 = P, \tilde{H}_0 = \tilde{H}, \tilde{H}_1 = \tilde{J}_+,$ and $\tilde{H}_2 = \tilde{J}_-$. The numerical solution of these three coupled equations determines all the necessary mean-field parameters for given values of the anisotropy and of the external magnetic field.

A. Mean-field phase diagram

The mean-field phase diagram (see Fig. 2) has already been discussed in Ref. 5. Here we would like to add some observations concerning the scaling limits $\gamma \rightarrow 0$ and $\gamma \rightarrow 1$, respectively. For small γ and $h < 1$ we may bosonize the

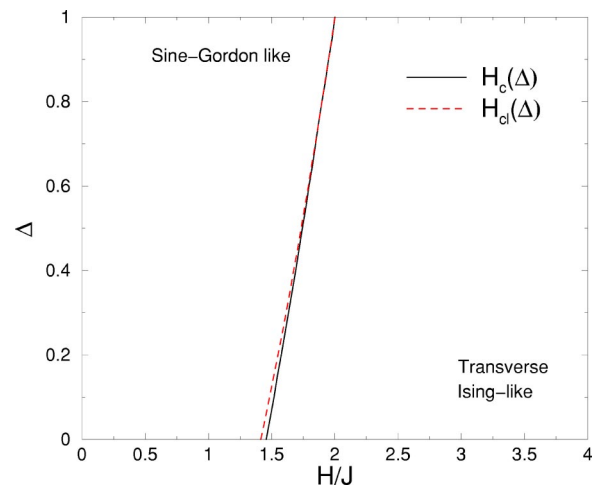


FIG. 2. Mean-field phase diagram. The critical line is denoted by $H_c(\Delta)$ and the classical line by $H_{ci}(\Delta)$.

mean-field Hamiltonian (8) and obtain a quantum sine-Gordon model, described by the Hamiltonian density

$$\mathcal{H} = \frac{v}{2} [(\partial_x \Theta)^2 + (\partial_x \Phi)^2] - \gamma \Lambda \cos \sqrt{4\pi} \Theta, \quad (14)$$

where Φ is a canonical Bose field and Θ its dual field, Λ is a constant, and $v = \tilde{J}_+ \sqrt{1-h^2}$ is the mean-field spin velocity at $\gamma=0$. For $h>1$ the $\gamma=0$ mean-field Hamiltonian has a ferromagnetic ground state and an excitation gap and bosonization cannot be carried out. The physics of the sine-Gordon model (SGM) (14) is very well understood. There are two elementary excitations known as soliton and antisoliton. The spectrum consists of scattering states of an even number of solitons and antisolitons. By solving the mean-field equations numerically we find that small γ is obtained for small fields H and goes to zero as $\Delta \rightarrow 1$ from below. This suggests that the physics of the mean-field theory at small fields is approximately described by the SGM. We note that for Δ slightly smaller than 1 it was shown in Ref. 11 that the full Hamiltonian (1) maps onto a sine-Gordon model. We elaborate on this fact in Sec. IV. For $\gamma \approx 1$ it is convenient to rewrite the Hamiltonian in terms of the real, fermionic operators

$$\eta_n = \sigma_n^x \prod_{j=1}^{n-1} \sigma_j^z, \quad \zeta_n = -i \prod_{j=1}^n \sigma_j^z \sigma_n^x. \quad (15)$$

Then one performs a rotation

$$\xi_{R,n} = \frac{\zeta_n + \eta_n}{\sqrt{2}}, \quad \xi_{L,n} = \frac{\zeta_n - \eta_n}{\sqrt{2}}, \quad (16)$$

and finally takes the continuum limit $\xi_{\alpha,n} \rightarrow \sqrt{a_0} \xi_{\alpha}(x)$. In this way one finds that Hamiltonian (8) reduces to

$$\mathcal{H} = -i \frac{v}{2} \int dx [\xi_R \partial_x \xi_R - \xi_L \partial_x \xi_L] - im \int dx \xi_R \xi_L, \quad (17)$$

where $\xi_{R,L}$ are right and left moving real (Majorana) fermions, respectively, and $v = \gamma \tilde{J}_+ a_0 / 2$, $m = (\tilde{J}_+ / 2)(h-1)$. The Majorana fermion theory (17) is the same as the continuum limit of the transverse field Ising model (TFIM), i.e., the mean-field Hamiltonian for $\gamma=1$, with a renormalized velocity. The elementary excitations are Z_2 kinks. The region $h < 1$ corresponds to the ordered phase, whereas $h > 1$ corresponds to the disordered phase of the TFIM. In the ordered phase the spin operator $\sigma(x)$ has a nonzero expectation value, which corresponds to the staggered magnetization in the underlying Heisenberg model. By solving the mean-field equations numerically we find that $\gamma \approx 1$ is only achieved for small $\Delta \approx 0$ and fields H that are significantly larger than H_c .

B. Staggered magnetization

Order in the system is represented by the staggered magnetization $m_{\text{st}} = \langle (-1)^j S_j^x \rangle$, which is obtained from Ref. 12 as

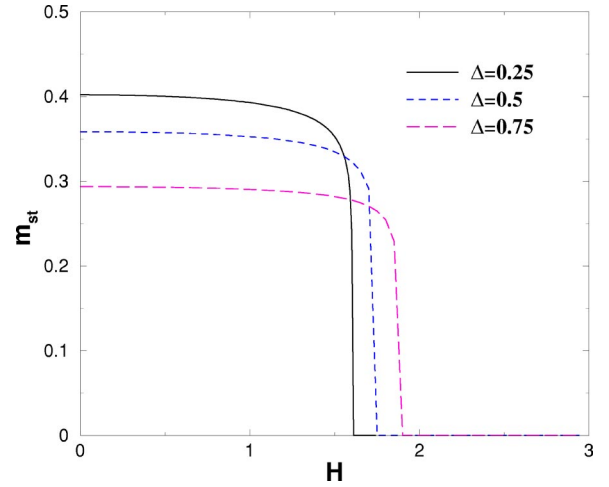


FIG. 3. Staggered magnetization as a function of external field for different anisotropies $\Delta=0.25, 0.5$, and 0.75 .

$$m_{\text{st}} = \begin{cases} \frac{(\tilde{J}_+ \tilde{J}_-)^{1/4} [1 - \tilde{H}^2 / \tilde{J}_+^2]^{1/8}}{(2(\tilde{J}_+ + \tilde{J}_-))^{1/2}}, & |\tilde{H}| < \tilde{J}_+ \\ 0, & |\tilde{H}| > \tilde{J}_+. \end{cases} \quad (18)$$

The mean-field result (18) becomes exact on the classical line $h_{cl} = \sqrt{2(1+\Delta)}$, where¹⁵ $m_{\text{st}} = \frac{1}{2} \sqrt{1 - (h_{cl}^2/4)}$. We plot m_{st} as a function of magnetic field for several values of Δ in Fig. 3.

C. Applicability of the mean-field approximation

It is immediately clear from the results for the staggered magnetization shown in Fig. 3 that the mean-field theory fails to describe model (1) in the limit of small applied magnetic fields H . In zero field Eq. (1) reduces to a critical XZX spin chain, for which the staggered magnetization vanishes. The XZX chain has a U(1) symmetry corresponding to rotations around the y axis, whereas the MFA breaks this symmetry and is therefore invalid. Simple scaling arguments suggest that in the limit $H \rightarrow 0$, m_{st} should be proportional to H^α , where the exponent α is a function of the anisotropy Δ .⁵ However, a renormalisation group analysis of the small H regime of Eq. (1) is nontrivial because in a bosonized description the transverse field carries conformal spin. We review some important features of this analysis in Sec. V.

In order to get some rough measure concerning the region of magnetic fields H in which the MFA may work well, we have computed the one-loop corrections to the mean-field values of values \mathcal{M} , K , and P . As there is no small parameter in the problem, this calculation should be understood as a semiclassical approximation. The corrections to \mathcal{M} , K , and P are obtained by taking partial derivatives of the correction to the ground state energy. The latter is found to be

$$\delta E_0 = \int_{-\pi}^{\pi} \frac{dpdqQ}{(2\pi)^3} \frac{\left[\frac{1}{2} F(p+Q, p) F(q+Q, q) \cos Q - F(p, q) F(p+Q, q+Q) \cos(p-q) \right] F(p+Q, p) F(q+Q, q) \cos Q}{\omega(p) + \omega(q) + \omega(p+Q) + \omega(q+Q)},$$

where $F(p, q) = \alpha_+(p)\alpha_-(q) + \alpha_-(p)\alpha_+(q)$. The corrections to the mean-field parameters \mathcal{M} , K , and P turn out to be quite small except for low fields and near the transition: as the gap becomes smaller, fluctuations become more important.

A better way to study the regime of applicability of the mean-field approximation is to compare some of its predictions to the results of numerical density matrix renormalization group (DMRG) calculations. Results for some values of Δ have been already been reported by Capraro and Gros in Ref. 13.

In Fig. 4 we compare DMRG results for the magnetization per site with the MFA for $\Delta=0.25$. We work with periodic boundary conditions and consider system sizes of up to 60 sites. The agreement between DMRG calculations and the MFA is quite satisfactory, particularly for sufficiently large fields $H \geq 1.2J$.

In Fig. 5 we compare DMRG results for the staggered magnetization per site with the MFA for $\Delta=0.25$. For $H < H_c$ the staggered magnetization is computed as

$$\langle 0 | S_n^x (-1)^n | 1 \rangle, \quad (19)$$

where $|0\rangle$ and $|1\rangle$ are the two degenerate ground states corresponding to momenta 0 and π , respectively. It is necessary to consider the overlap (19), because, in a finite volume with periodic boundary conditions, translational invariance implies that

$$\langle 0 | S_n^x (-1)^n | 0 \rangle = \langle 1 | S_n^x (-1)^n | 1 \rangle = 0. \quad (20)$$

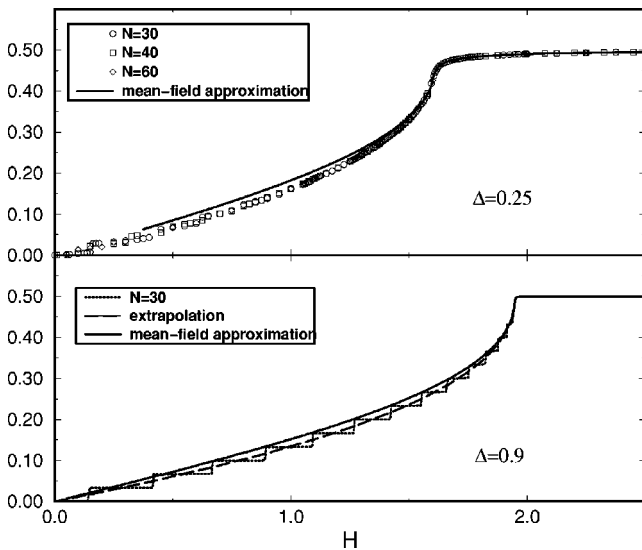


FIG. 4. Magnetization per site calculated from the MFA compared to the results of DMRG computations for $\Delta=0.25$.

In the infinite volume translational invariance is spontaneously broken and the ground state becomes a linear combination of $|0\rangle$ and $|1\rangle$. We note that the finite-size effects for weak and strong fields are still rather pronounced. Such a behavior for the staggered magnetization in finite systems was previously observed in, e.g., Ref. 14. Nevertheless it is clear that the staggered magnetization vanishes above a critical field and approaches zero in the weak field limit. The agreement between the DMRG results and the MFA for weak fields is as expected quite poor. For sufficiently large field $H \geq 1.2J$ the MFA gives good results. Last but not least we have used the DMRG to determine the gaps of the two lowest lying excited states. The results are shown in Fig. 6. Both gaps vanish at the critical field H_c . For $H < H_c$ the first excited state is really a degenerate ground state with the opposite sign of the staggered magnetization. This degeneracy is removed in the thermodynamic limit by spontaneous symmetry breaking. Hence the true excitation gap is given by the second excited state. We see that the MFA is in very good agreement with the DMRG results for fields that are larger than approximately $1.5J$. This is only slightly below the critical field H_c .

The above considerations suggest that the MFA works very well for both ground state and excited states properties as long as the applied field is sufficiently strong $H \geq 1.5J$. For intermediate field strengths $0.5J \leq H \leq 1.5J$ we expect the MFA to give at least qualitatively correct results. In the small-field regime the MFA gives very poor results and fails completely in the limit $H \rightarrow 0$. Having in mind these limitations we will now determine the dynamical structure factor in the MFA.

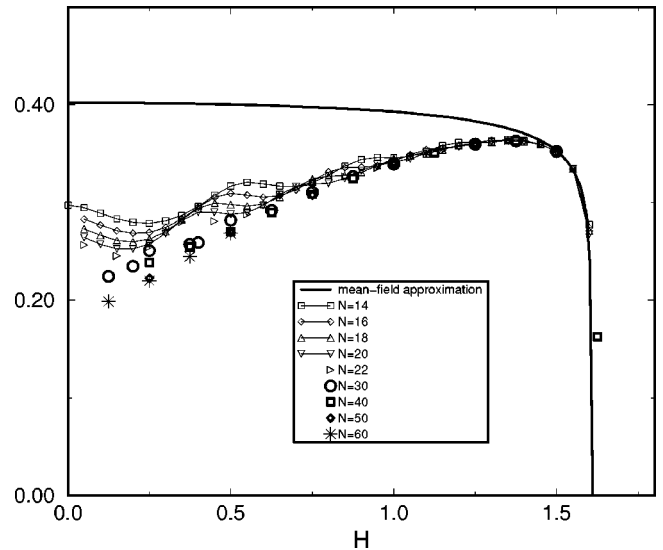


FIG. 5. Staggered magnetization calculated from the MFA compared to the results of DMRG computations for $\Delta=0.25$.

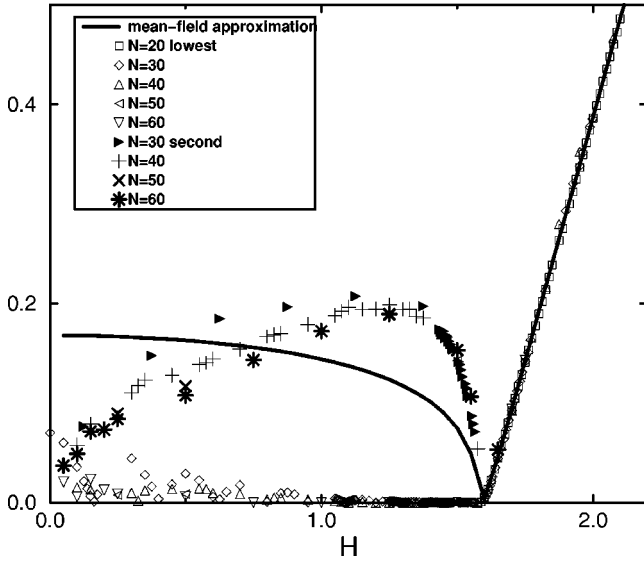


FIG. 6. Excitation gap calculated from the MFA compared to the results of DMRG computations for $\Delta=0.25$.

III. DYNAMICAL STRUCTURE FACTOR IN THE MEAN-FIELD APPROXIMATION

The transverse correlators are determined in the framework of the mean-field theory as follows. Let us denote the true ground state by $|0\rangle$ and the mean-field ground state by $|0\rangle_{\text{MF}}$. Then we employ the following approximation:

$$\begin{aligned} \langle 0|S_n^\alpha(t)S_m^\beta|0\rangle &= \langle 0|e^{iH_0 t}S_n^\alpha e^{-iH_0 t}S_m^\beta|0\rangle \\ &\approx_{\text{MF}} \langle 0|e^{iH_{xy} t}S_n^\alpha e^{-iH_{xy} t}S_m^\beta|0\rangle_{\text{MF}}. \end{aligned} \quad (21)$$

In other words we replace the ground state expectation value by the expectation value with respect to the mean-field ground state and substitute the xy Hamiltonian (8) for the full Hamiltonian in the time evolution operator. It is clear that Eq. (21) will be a good approximation as long as the mean-field theory gives an accurate description of the ground state and low-lying excited states. The transverse spin correlators in theory (8) have been determined as a spectral sum over intermediate multiparticle states in Refs. 7–9.

A. Transverse correlations in the “low-field phase”: $h < 1$

For $h < 1$, the leading contribution comes from two-particle intermediate states. As a result all components of the structure factor are completely incoherent. The other contributions are due to states with 4, 6, ... particles, but they are expected to contribute less spectral weight so that we ignore them here. The two-particle contributions to the structure factor are given by

$$\begin{aligned} S^{\alpha\beta}(\omega, k) &= \int_{-\pi}^{\pi} \frac{dk_1 dk_2}{2\pi} \delta(\omega - \omega(k_1) - \omega(k_2)) \\ &\quad \times \delta(k - k_1 - k_2 + \pi) g_{\alpha\beta}(k_1, k_2). \end{aligned} \quad (22)$$

Here

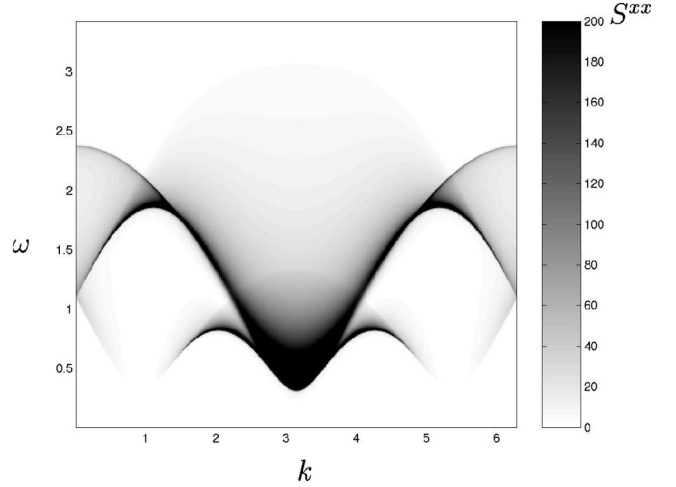


FIG. 7. Structure factor S^{xx} as a function of k and ω for anisotropy $\Delta=0.25$ and external magnetic field $H=0.8J$.

$$\begin{aligned} g_{xx}(k_1, k_2) &= \frac{C(1+\gamma)^{-1}}{8[1-\cos(k_1+k_2)]} \frac{[\omega(k_1) - \omega(k_2)]^2}{\omega(k_1)\omega(k_2)}, \\ g_{yy}(k_1, k_2) &= \frac{C(1+\gamma)}{8} \frac{1-\cos(k_1-k_2)}{\omega(k_1)\omega(k_2)} \tilde{J}_+^2, \\ g_{xy}(k_1, k_2) &= i \frac{C}{8} \frac{\sin\left(\frac{k_1-k_2}{2}\right)}{\sin\left(\frac{k_1+k_2}{2}\right)} \left[\frac{\tilde{J}_+}{\omega(k_1)} - \frac{\tilde{J}_+}{\omega(k_2)} \right], \end{aligned} \quad (23)$$

where $C = [\gamma^2(1-h^2)]^{1/4}$ and where we have corrected a typo in Ref. 9. The result for g_{xy} is a conjecture based on calculations we have performed in the Ising and sine-Gordon scaling limits and agrees with the known result on the classical line.¹⁵ We note that the results for $S^{\alpha\alpha}(\omega, k)$ reduce to the exact results¹⁵ for model (8) on the classical line as well, which implies that all multiparticle matrix elements vanish. We see that the two-particle contribution to the off-diagonal element $S^{xy}(\omega, k)$ is purely imaginary. This means that it cannot be seen in neutron scattering experiments as it enters expression (2) for the intensity in the form

$$\left(\delta_{\alpha\beta} - \frac{k_x k_y}{\mathbf{k}^2} \right) [S^{xy}(\omega, k) + S^{yx}(\omega, k)], \quad (24)$$

where we recall that $k = \mathbf{k} \cdot \mathbf{e}$ is the component of the momentum transfer along the chain direction. Using the relation

$$S^{yx}(\omega, k) = (S^{xy}(\omega, k))^*, \quad (25)$$

we see that $S^{xy}(\omega, q) + S^{yx}(\omega, q)$ is zero whenever S^{xy} is purely imaginary.

The intensity of the structure factor $S^{\alpha\alpha}$ is plotted as a function of k and ω in Figs. 7–10 for anisotropy $\Delta=0.25$ and for external magnetic fields $H=0.8J$ and $H=1.4J$, corresponding to the effective mean-field values $h=0.44$ and 0.82 , respectively. It follows from our discussion in Sec. II C that we do not expect the results for $h=0.44$ to provide a

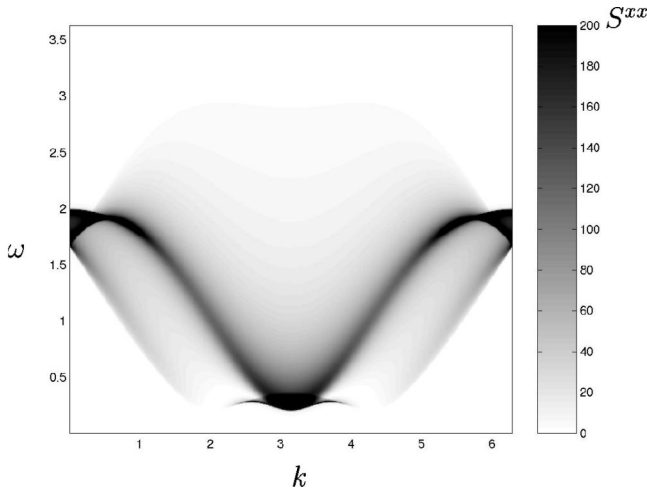


FIG. 8. Structure factor S^{xx} as a function of k and ω for anisotropy $\Delta=0.25$ and external magnetic field $H=1.4J$.

quantitative description of the structure factor of the transverse field XXZ chain. However the mean-field approximation may still capture the redistribution of spectral weight in the various components of the structure factor as the transverse field is increased on a qualitative level. One clearly sees in, e.g., Fig. 7 that the magnetic field splits the lower boundary into two branches. Experimentally, one would thus expect to see a double peak in the intensity when scanning in frequency for fixed momentum. In Fig. 8, the evolution of the structure factor with increasing magnetic field can be seen: the branches recollapse around $k=\pi$, with diminishing gap (the gap vanishes at $H_c=1.604J$, corresponding to $h=1$). As the field gets closer to the critical field, the intensity of the structure factor collapses from an incoherent continuum onto an emergent single coherent mode.

B. Transverse correlations in the “high-field phase”: $h>1$

For fields $h>1$ the dominant contribution to the dynamical structure factor is due to a single-particle coherent mode with a dispersion relation given by Eq. (12). We have⁷⁻⁹

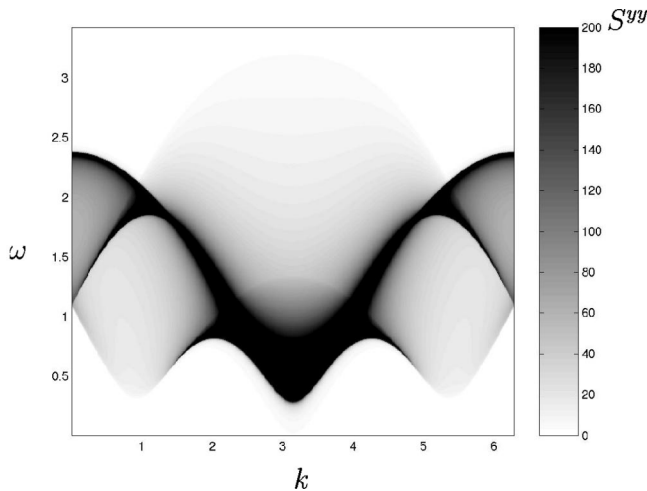


FIG. 9. Structure factor S^{yy} as a function of k and ω for anisotropy $\Delta=0.25$ and external magnetic field $H=0.8J$.

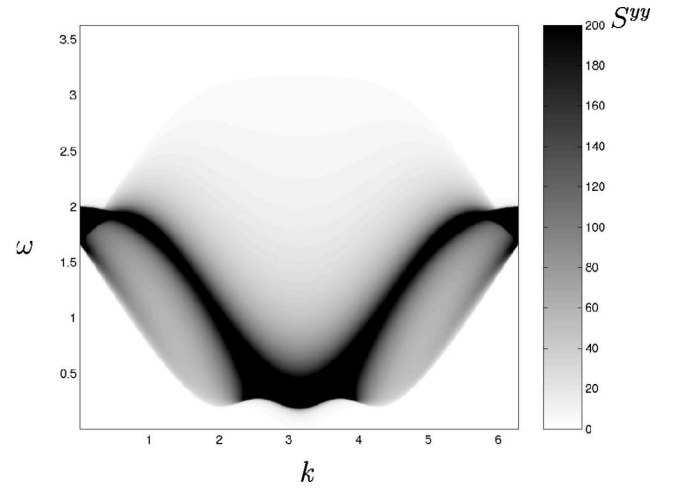


FIG. 10. Structure factor S^{yy} as a function of k and ω for anisotropy $\Delta=0.25$ and external magnetic field $H=1.4J$.

$$S^{\alpha\beta}(\omega, k) = f_{\alpha\beta}(k - \pi) \delta(\omega - \omega(k)), \quad (26)$$

where

$$\begin{aligned} f_{xx}(k) &= \frac{\rho_\infty}{[A(k)]}, & f_{yy}(k) &= \rho_\infty A(k), \\ f_{xy}(k) &= -i\rho_\infty, & f_{xz}(k) &= f_{yz}(k) = 0. \end{aligned} \quad (27)$$

Here we have introduced the parameters

$$\begin{aligned} \lambda_{1,2} &= \frac{h \pm \sqrt{h^2 + \gamma^2 - 1}}{1 - \gamma}, \\ \rho_\infty &= \frac{1}{4} [(1 - \lambda_2^2)(1 - \lambda_1^{-2})(1 - \lambda_2 \lambda_1^{-1})]^{1/4}, \end{aligned} \quad (28)$$

$$A(k) = \left[\frac{\lambda_2^2 - 2\lambda_2 \cos(k) + 1}{\lambda_1^{-2} - 2\lambda_1^{-1} \cos(k) + 1} \right]^{1/2}.$$

We note that f_{xy} is purely imaginary, which again means that the mixed correlations cannot be observed in neutron scattering experiments.

Near the transition, the amplitude f_{xx} diverges at $k=\pi$. For fields higher than the critical field, the divergence is smoothed out, as can be seen in Fig. 11. The gap also reopens, as can be seen from Eq. (12).

C. Longitudinal correlations

The longitudinal correlation function S^{zz} can be computed directly in terms of a density-density correlator of the c fermions. After the BdG transformation to c' Fermions, a straightforward vacuum expectation value yields¹⁰

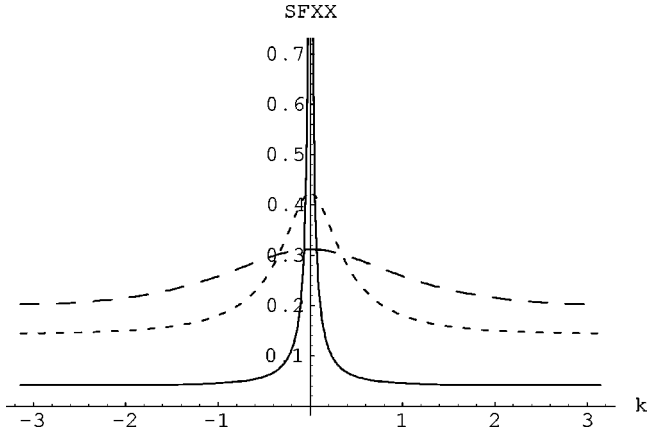


FIG. 11. f^{xx} structure factor amplitude as a function of k for external magnetic fields $H=1.604$, 1.7 , and 2.4 (above the critical field). This is the amplitude of the structure factor along the dispersion relation δ function.

$$S^{zz}(\omega, k) = \int_0^\pi \frac{dq}{4\pi} [1 - f(q, k)] \delta(\omega - \omega(q, k)),$$

$$f\left(q + \frac{k}{2}, k\right) = \frac{a(q)a(q+k) - b(q)b(q+k)}{\omega(q)\omega(q+k)}, \quad (29)$$

$$\omega(q, k) = \omega(q - k/2) + \omega(q + k/2),$$

where $a(k) = \tilde{J}_+ \cos(k) + \tilde{H}$ and $b(k) = \tilde{J}_- \sin(k)$. Equations (29) are valid in both the low-field and in the high-field phase. As a result, the longitudinal correlations are incoherent for any value of the applied magnetic field.

The evolution of S^{zz} with increasing applied field H is shown in Figs 12 and 13. First, the longitudinal correlations are generally incommensurate. Second, in low fields the intensity is concentrated at the upper boundary of the continuum, as is expected as Δ is small, whereas for larger fields a shift towards lower energies is visible.

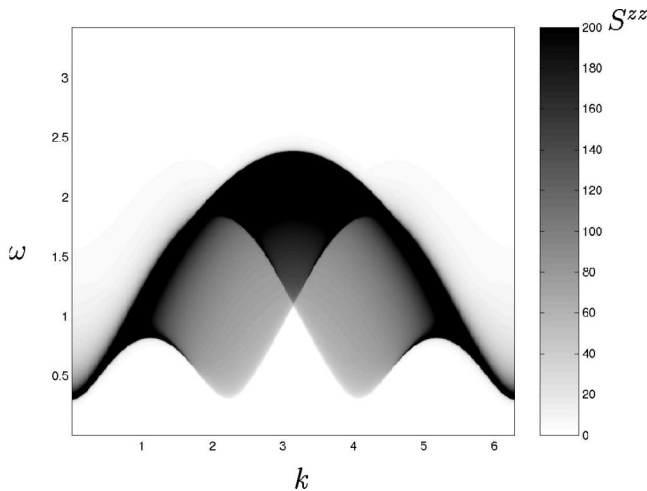


FIG. 12. Structure factor S^{zz} as a function of k and ω for anisotropy $\Delta=0.25$ and external magnetic field $H=0.8J$.

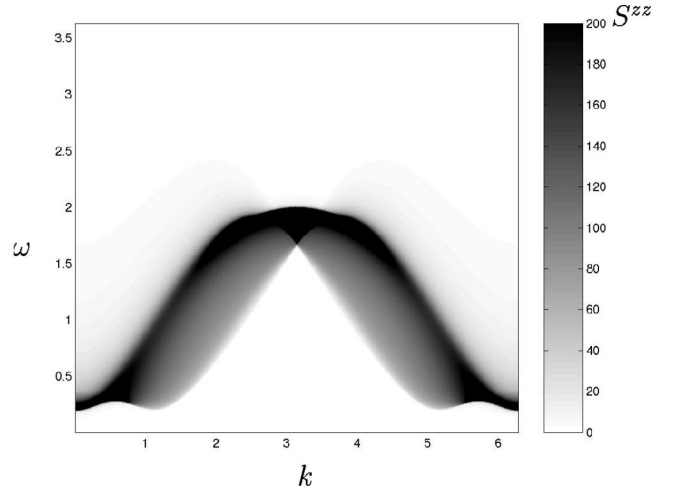


FIG. 13. Structure factor S^{zz} as a function of k and ω for anisotropy $\Delta=0.25$ and external magnetic field $H=1.4J$.

IV. FIELD THEORY APPROACH TO THE SMALL-ANISOTROPY LIMIT

The easiest case to deal with by field theory methods is the one where the magnetic field H is much stronger than the anisotropy $1 - \Delta$. The field theory limit in this case was studied in Ref. 11 and subsequently in Ref. 16. Let us consider the Hamiltonian

$$\mathcal{H}_{\text{ZXX,H}} = J \sum_{j,\alpha} S_j^\alpha S_{j+1}^\alpha + H \sum_j S_j^z + (\Delta - 1) S_j^y S_{j+1}^y$$

$$\equiv \mathcal{H}_0 + \mathcal{H}_1. \quad (30)$$

As we assume the field H to be much larger than the anisotropy $1 - \Delta$, we bosonize at the point $\Delta=1$ in the presence of a strong field and then switch on the exchange anisotropy as a perturbation.

At low energies \mathcal{H}_0 is described by a free massless boson compactified on a ring of radius R , i.e., Φ and $\Phi + 2\pi R$ are identified. The dual field Θ fulfills $\Theta = \Theta + 1/R$. The bosonization rules are

$$\vec{S}_n \rightarrow \vec{J}(x) + (-1)^n \vec{n}(x) + \text{higher harmonics}, \quad (31)$$

where a_0 is the lattice spacing, $x = na_0$ and

$$J^x = b \cos[\beta\Theta(x)] \sin\left(\frac{2\pi}{\beta}\Phi(x) - 2\delta x\right),$$

$$J^y = -b \sin[\beta\Theta(x)] \sin\left(\frac{2\pi}{\beta}\Phi(x) - 2\delta x\right),$$

$$J^z = \frac{a_0}{\beta} \partial_x \Phi(x), \quad (32)$$

$$n^x(x) = c \cos[\beta\Theta(x)], \quad n^y(x) = c \sin[\beta\Theta(x)],$$

$$n^z(x) = a \sin\left(\frac{2\pi}{\beta}\Phi(x) - 2\delta x\right).$$

Here $\beta = 2\pi R$ and the coefficients a, c are known exactly in the absence of a magnetic field¹⁷ and numerically for several values of the applied field H .^{18,19} The (magnetic-field dependent) constant β , the incommensurability δ and spin velocity $v_s(H)$ are determined by the microscopic parameters Δ, J and H of the lattice model by using the exact Bethe ansatz solution. This entails solving some linear integral equations numerically (see, e.g., Refs. 11 and 20–22). The bosonization formulas (32) hold as long as $H < 2J$. For $H > 2J$ the ground state of \mathcal{H}_0 is the saturated ferromagnetic state and the excitation spectrum is gapped. For later convenience we define

$$\xi = \frac{4\beta^2}{8\pi - 4\beta^2}. \quad (33)$$

The perturbing Hamiltonian \mathcal{H}_1 can now be bosonized using Eq. (32) and fusion of the staggered magnetizations n^y gives a contribution proportional to

$$\cos(2\beta\Theta). \quad (34)$$

In addition there is a small marginal contribution that shifts the compactification radius. For simplicity we neglect it here.

Thus, at low energies compared to the scale set by the applied field $H < 2J$, the effective Hamiltonian is given by a sine-Gordon model

$$\mathcal{H} = \frac{v_s}{2} [(\partial_x \Phi)^2 + (\partial_x \Theta)^2] - \mu(\Delta) \cos(2\beta\Theta). \quad (35)$$

The cosine term in the sine-Gordon model is relevant and generates a spectral gap. As $2\beta > \sqrt{4\pi}$ (see, e.g., Fig. 1 of Ref. 20), the spectrum of the sine-Gordon model consists of soliton and antisoliton only. We can immediately read off the scaling of the gap as a function of $1 - \Delta$:

$$M \propto (1 - \Delta)^{\pi/(2\pi - \beta^2)}. \quad (36)$$

The magnetic field dependence enters both via the prefactor and via the H dependence of β . In order to calculate the prefactor as well as quantities like the magnetization we need to know the normalization of the operator

$$\mathcal{O}_j = S_j^y S_{j+1}^y \rightarrow -\mathcal{C} \cos(2\beta\Theta) \quad (37)$$

in the Heisenberg chain in a field, i.e., Hamiltonian (30) with $\Delta = 1$. At present the normalization \mathcal{C} is not known. In Ref. 19 the issue of how to determine \mathcal{C} from the large-distance asymptotics of appropriately chosen correlation functions in the Heisenberg chain in a uniform field has been investigated. In what follows we will consider \mathcal{C} as a yet unknown function of the magnetic field H . The gap is given by

$$\frac{M}{J} = \frac{2\tilde{v}}{\sqrt{\pi}} \frac{\Gamma\left(\frac{\eta}{2-2\eta}\right)}{\Gamma\left(\frac{1}{2-2\eta}\right)} \left(\frac{(1-\Delta)\mathcal{C}\pi}{2\tilde{v}} \frac{\Gamma(1-\eta)}{\Gamma(\eta)} \right)^{1/(2-2\eta)}, \quad (38)$$

where

$$\eta = \beta^2/2\pi, \quad (39)$$

and \tilde{v} is the dimensionless spin velocity

$$\tilde{v} = \frac{v_s}{Ja_0}. \quad (40)$$

The staggered magnetization in the x direction is nonzero in the presence of a transverse field. We have

$$\langle (-1)^n S_n^x \rangle = c \langle \cos \beta\Theta \rangle, \quad (41)$$

where²³

$$\begin{aligned} & \langle \cos \beta\Theta \rangle \\ &= \left[\frac{M \sqrt{\pi} \Gamma\left(\frac{1}{2-2\eta}\right)}{2\tilde{v}J \Gamma\left(\frac{\eta}{2-2\eta}\right)} \right]^{\eta/2} \\ & \times \exp \left[\int_0^\infty dt \left(\frac{\sinh(\eta t)}{2 \sinh(t) \cosh([1-\eta]t)} - \frac{\eta}{2} e^{-2t} \right) \right]. \end{aligned} \quad (42)$$

The magnetization per site can be calculated from the ground state energy of the Hamiltonian by taking derivatives with respect to the magnetic field H . The total ground state energy per site is given by

$$e_{\text{tot}}(H) = e_{\text{XXX}}(H) + e_{\text{SG}}(H, \Delta), \quad (43)$$

where the ground state energy per site of the isotropic Heisenberg lattice model $e_{\text{XXX}}(H)$ is known exactly from the Bethe Ansatz (see, e.g., Ref. 21) and where e_{SG} is the ground state energy of the sine-Gordon model²⁴

$$e_{\text{SG}}(H, \Delta) = -\frac{M^2}{4\tilde{v}J} \tan\left(\frac{\pi\xi}{2}\right). \quad (44)$$

The magnetization is given by

$$m = \frac{\partial e_{\text{tot}}(H)}{\partial H} = m_{\text{XXX}} + \frac{\partial e_{\text{SG}}(H, \Delta)}{\partial H}. \quad (45)$$

The only unknown in the expression for the staggered magnetization (41) and magnetization (45) is the normalization \mathcal{C} in (37). Once this is known with sufficient accuracy for taking derivatives with respect to H both m and $\langle (-1)^n S_n^x \rangle$ can be evaluated.

Dynamical structure factor

Using the integrability of the SGM it is possible to evaluate the low-energy asymptotics of dynamical correlation functions. Let us start with the transverse correlations and concentrate on momenta close to π/a_0 . The staggered magnetizations in x and y directions are given by Eqs. (32) and calculating their correlation functions reduces to the calculation of particular correlators in the SGM. This is by now a standard calculation (see, e.g., Ref. 20): one determines the first few terms in a Lehmann representation by using the

exact matrix elements²⁵ of the operator under consideration between the ground state and (multi) soliton/antisoliton excited states. The leading contribution is due to intermediate states with one soliton and one antisoliton. Using the notations of Ref. 26 we obtain

$$S^{yy}\left(\omega, \frac{\pi}{a_0} + k\right) = \frac{2\tilde{v}Jc^2}{\pi s\sqrt{s^2 - 4M^2}} \left| \frac{\mathcal{G}_\beta G(2\theta_0)/C_1}{\xi \cosh\left(\frac{2\theta_0 + i\pi}{2\xi}\right)} \right|^2 \times \Theta_H\left(\frac{s}{M} - 2\right) + \text{contrib. from 4,6, \dots particles,} \quad (46)$$

where $\Theta_H(x)$ is the Heaviside function, s and θ_0 are defined as

$$s = \sqrt{\omega^2 - v_s^2 k^2}, \quad \theta_0 = \text{arccosh}\left(\frac{s}{2M}\right), \quad (47)$$

and \mathcal{G}_β and $G(\theta)$ are given by

$$G(\theta) = iC_1 \sinh(\theta/2) \times \exp\left[\int_0^\infty \frac{dt}{t} \left(\frac{\sinh^2(t[1 - i\theta/\pi]) \sinh(t[\xi - 1])}{\sinh(2t) \sinh(\xi t) \cosh(t)} \right)\right],$$

$$\mathcal{G}_\beta = \left[\frac{M\sqrt{\pi}}{2\tilde{v}J} \frac{\Gamma\left(\frac{1}{2-2\eta}\right)}{\Gamma\left(\frac{\eta}{2-2\eta}\right)} \right]^{\eta/2} \times \exp\left[\int_0^\infty \frac{dt}{t} \left(\frac{\sinh \eta t}{2 \sinh(t) \cosh([1-\eta]t)} - \frac{\eta}{2} e^{-2t} \right)\right], \quad (48)$$

where

$$C_1 = \exp\left[-\int_0^\infty \frac{dt}{t} \frac{\sinh^2(t/2) \sinh(t[\xi - 1])}{\sinh 2t \sinh \xi t \cosh t}\right]. \quad (49)$$

The analogous result for $S^{xx}[\omega, (\pi/a_0) + k]$ is

$$S^{xx}\left(\omega, \frac{\pi}{a_0} + k\right) = \frac{2\tilde{v}Jc^2}{\pi s\sqrt{s^2 - 4M^2}} \left| \frac{\mathcal{G}_\beta G(2\theta_0)/C_1}{\xi \sinh\left(\frac{2\theta_0 + i\pi}{2\xi}\right)} \right|^2 \times \Theta_H\left(\frac{s}{M} - 2\right) + \text{contrib. from 4,6, \dots particles.} \quad (50)$$

Finally we determine the longitudinal structure factor $S^{zz}(\omega, k)$ by making use of recent results by Lukyanov and Zamolodchikov.²⁷ It is clear from the bosonization formulas (32) that the correlations of n^z are incommensurate. In other words the longitudinal structure factor has low-energy modes at the incommensurate momenta $\pi/a_0 \pm 2\delta$. Moreover one can easily establish that the operators

$$\exp\left(\pm i \frac{2\pi}{\beta} \Phi\right), \quad (51)$$

have topological charges of ∓ 2 , respectively. Here the operator of the topological charge is defined as

$$Q = \frac{\beta}{\pi} \int_{-\infty}^{\infty} dx \partial_x \Theta(x). \quad (52)$$

The leading contribution to the longitudinal spin-spin correlation functions is due to intermediate states with two solitons or two antisolitons. The form factors of vertex operators like Eq. (51) with definite topological charges have been given in Ref. 27. A short calculation leads to the following result:

$$S^{zz}\left(\omega, \frac{\pi}{a_0} \pm 2\delta + k\right) = \frac{\tilde{v}Ja^2 Z_2(0)}{4\pi s\sqrt{s^2 - 4M^2}} |G(2\theta_0)|^2 \Theta_H\left(\frac{s}{M} - 2\right) + \text{contrib. from 4,6, \dots particles.} \quad (53)$$

The normalization $Z_2(0)$ is

$$Z_2(0) = \frac{8}{\xi C_1^2} \left[\frac{\sqrt{\pi} M \Gamma\left(\frac{3}{2} + \frac{\xi}{2}\right)}{J\tilde{v}\Gamma\left(\frac{\xi}{2}\right)} \right]^{2\pi/\beta^2} \times \exp\left[\int_0^\infty \frac{dt}{t} \left(\frac{\cosh(t) - \exp(-[1+\xi]t)}{\sinh(\xi t) \cosh(t)} - \frac{2\pi e^{-2t}}{\beta^2} \right)\right], \quad (54)$$

where C_1 is given in Eq. (49). The structure factor depends on the transverse field both through the gap M and through the parameter 2β . The variation of 2β does not alter the various components of the dynamical structure factor on a qualitative level: the leading contributions are always due to two particles; the structure factor is entirely incoherent and always vanishes at the threshold (as 2β is always strictly larger than $\sqrt{4\pi}$), which occurs at $\omega = 2M$. However, on a quantitative level the value of β is quite important: decreasing β leads to a narrowing of the lineshape in the transverse correlations. What we mean precisely by this is illustrated in Fig. 14, where we plot $J(M/J)^{2-\eta} S^{yy}(\omega, \pi/a_0)$ as a function of ω/M for several values of the magnetic field H . We see that the lineshape, when measured in units of the field-dependent gap M , sharpens with increasing magnetic field H . However, as M itself depends on H , this does not necessarily imply that the lineshape measured in physical units like meV sharpens with increasing H . It is somewhat difficult to compare our field theory results to the ones obtained in the mean-field approximation as we have no reliable way of determining the gap M .

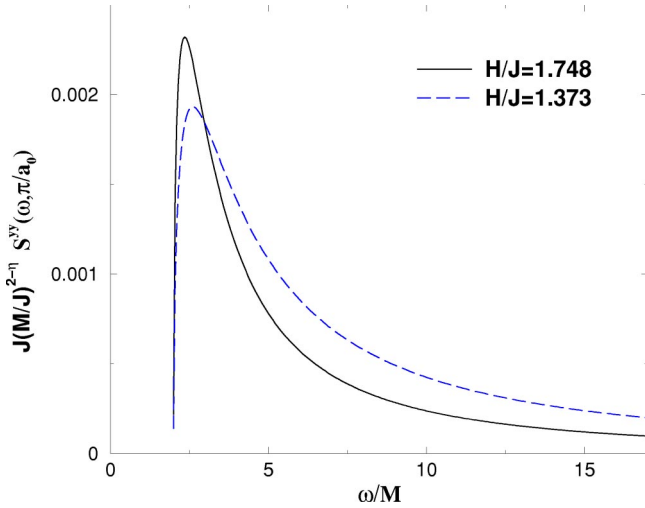


FIG. 14. $J(M/J)^{2-\eta} S^{yy}(\omega, \pi/a_0)$ as a function of ω/M for $H = 1.373J$ and $H = 1.748J$, corresponding to a magnetization per site of 0.2 and 0.3, respectively. The scales of both x and y axes depends on H through the gap M .

V. FIELD THEORY APPROACH TO THE WEAK FIELD LIMIT

The situation where the field is weak compared to the anisotropy, i.e., $H \ll (1 - \Delta)$, has been analyzed by renormalization group methods by Nersesyan *et al.* in Ref. 28. It is convenient to rotate the quantization axis such that the anisotropy is in the z direction and the field is along the x direction. The effect of the magnetic field is to generate an excitation gap and a nonzero expectation value for the staggered magnetization in the y direction. This can be seen as follows. The chain Hamiltonian is

$$\begin{aligned} \mathcal{H}_{XXZ,H} &= J \sum_j S_j^x S_{j+1}^x + S_j^y S_{j+1}^y + \Delta S_j^z S_{j+1}^z + H \sum_j S_j^x \\ &= \mathcal{H}_0 + \mathcal{H}_1, \end{aligned} \quad (55)$$

where \mathcal{H}_0 is the Hamiltonian of the anisotropic spin-1/2 chain and

$$\mathcal{H}_1 = H \sum_j S_j^x. \quad (56)$$

What we do now is to bosonize at the critical point defined by \mathcal{H}_0 , i.e., the anisotropic Heisenberg chain, and then to perturb away from this fixed point theory by Eq. (56). The bosonized form of \mathcal{H}_0 is

$$\mathcal{H}_0 = \frac{v_s}{2} \int dx [(\partial_x \Theta)^2 + (\partial_x \Phi)^2], \quad (57)$$

where Φ is a canonical bosonic field and Θ is the dual field. The perturbing operator is given by

$$\mathcal{H}_1 = \frac{bH}{a_0} \int dx \left[\cos(\beta\Theta) \sin\left(\frac{2\pi}{\beta}\Phi\right) \right], \quad (58)$$

where

$$\beta = \sqrt{2\pi - 2 \arccos(\Delta)}. \quad (59)$$

The perturbing operator (58) is *formally relevant*, but as it is not a Lorentz scalar it requires special treatment. As has been shown explicitly for the case $\Delta=0$ in Ref. 28 the Hamiltonian (55) can be related to a two chain model of spinless Luttinger liquids coupled by a weak interchain hopping. The generalization to $0 \leq \Delta < 1$ is straightforward. In order to match the notations of Ref. 28 we perform a shift

$$\Phi(x) \rightarrow \Phi(x) + \frac{\beta}{4}, \quad (60)$$

while keeping the dual field unchanged. The one-loop renormalization group (RG) analysis can then be read off from Refs. 28 and 29. At second order in the coupling the following two scalar operators are generated radiatively

$$\cos(2\beta\Theta), \quad \cos\left(\frac{4\pi}{\beta}\Phi\right). \quad (61)$$

Altogether we thus have three perturbing operators with corresponding dimensionless couplings z (of $\cos(\beta\Theta)$), g_1 (of $-\cos(4\pi/\beta\Phi)$) and g_2 [of $-\cos(2\beta\Theta)$]. The RG equations read^{28,29}

$$\frac{dz}{dl} = \left[2 - \frac{1}{2} \left(\eta + \frac{1}{\eta} \right) \right] z,$$

$$\frac{dg_1}{dl} = 2 \left(1 - \frac{1}{\eta} \right) g_1 - \left(\eta - \frac{1}{\eta} \right) z^2, \quad (62)$$

$$\frac{dg_2}{dl} = 2(1 - \eta)g_2 + \left(\eta - \frac{1}{\eta} \right) z^2,$$

$$\frac{d \ln \eta}{dl} = -\frac{1}{2} \left(g_2^2 \eta - \frac{g_1^2}{\eta} \right),$$

where

$$\eta(0) = \frac{\beta^2}{2\pi} = 1 - \frac{1}{\pi} \arccos(\Delta). \quad (63)$$

In general these equations have to be solved numerically. However, in the case $\eta(0) \approx 1$, i.e., a small exchange anisotropy, one can analyze the equations by a two-cutoff scaling procedure.²⁸ This is because z reaches strong coupling while $g_{1,2}$ remain small. The gap can then be estimated as

$$M \propto H \exp\left(-\frac{\pi}{4 - 4\eta(0)}\right). \quad (64)$$

The gap is linear in H , but the coefficient is very small as $\eta(0) \approx 1$. As is also shown in Ref. 28, at the point l_0 in the RG flow where z stops renormalizing the Hamiltonian is given by

$$\begin{aligned} \mathcal{H} = & \frac{v_s}{2} \int dx [(\partial_x \Theta)^2 + (\partial_x \Phi)^2] \\ & + \frac{g \pi v_s}{(2 \pi a_0)^2} \int dx [\cos(\sqrt{8 \pi / \eta} \Phi) - \cos(\sqrt{8 \pi \eta} \Theta)], \end{aligned} \quad (65)$$

where

$$g = 2 \frac{1 - \eta^{-2}}{1 + \eta^2} < 0. \quad (66)$$

As $\eta < 1$, the first cosine term is irrelevant and can be dropped. The Θ field gets pinned at the value $\pi/2\beta$, which implies that the staggered magnetization in the y direction is nonzero:

$$\langle (-1)^n S_n^y \rangle \propto \langle \sin \beta \Theta \rangle = \text{const}. \quad (67)$$

If Δ is not close to 1, the RG equations (62) have to be integrated numerically. Now several couplings grow simultaneously. Eventually η becomes very small, while g_2 becomes very large and negative. This means that we again flow toward a sine-Gordon model for the dual field and by the same argument as before we find that the staggered magnetization in the y direction is nonzero.

VI. DISCUSSION AND CONCLUSIONS

As discussed recently in Ref. 4, Cs_2CoCl_4 is a quasi-one-dimensional spin-3/2 antiferromagnet with a strong single-ion anisotropy D . At energies small compared to D the spin degrees of freedom are described by the anisotropic spin-1/2 Heisenberg model (1).⁴ Due to the smallness of the exchange constant ($J=0.23$ meV) it is possible to perform inelastic neutron scattering experiments in magnetic fields that are fairly large compared to J . Hence it should be possible to explore much of the magnetic phase diagram experimentally.

Our analysis suggests that at low fields $H < H_c$, all components of the dynamical structure factor are incoherent and the leading contributions come from intermediate states with two particles. These particles are different from the spinons of the critical XZX chain in that they are gapped and do not carry any definite spin (S^z is not a good quantum number). In a simple picture these particles have an interpretation as domain walls between the two possible antiferromagnetic spin alignments in the x direction. An argument in favor of this qualitative picture may be obtained by considering the classical line. Here it has been shown in Refs. 3 and 15 that the ground state is twofold degenerate. The expectation values of the staggered magnetization in the two ground states differ by an overall minus sign. This suggests that low-lying excitations can be loosely thought of as domain walls between the two possible ground states.

For high fields, the zz component of the dynamical structure factor remains incoherent, whereas the xx , xy , and yy components now feature a single-particle coherent mode. For very large fields and small Δ this particle is similar in nature to the Z_2 kinks of the transverse field Ising model in the

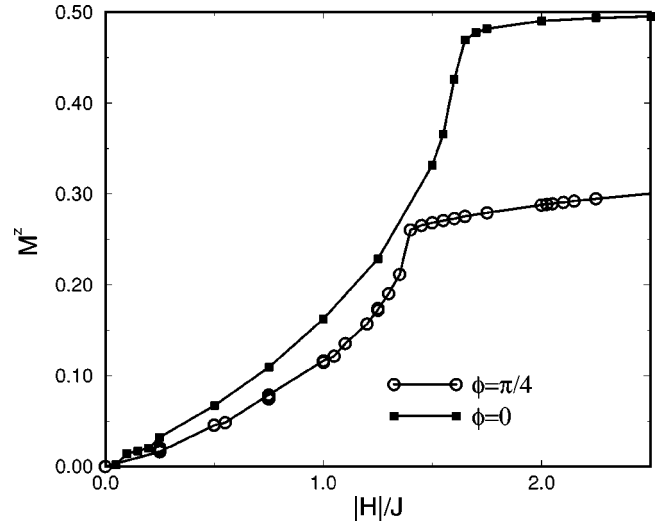


FIG. 15. DMRG results for the magnetization in the z direction for a magnetic field applied in the yz plane at a $\phi=45^\circ$ angle to the y axis. The results for a purely transverse field $\phi=0$ are shown for comparison.

strong field limit. A physical picture of these excitations is presented in Ref. 30. It would be interesting to compare our results for the dynamical structure factor to inelastic neutron scattering experiments on Cs_2CoCl_4 or similar compounds.

An interesting question which we have not addressed is what happens when the magnetic field is applied at an arbitrary angle to the exchange anisotropy. The most general case is given by

$$\mathcal{H} = J \sum_j \mathbf{S}_j \cdot \mathbf{S}_{j+1} + (\Delta - 1) S_j^y S_{j+1}^y + \mathbf{H} \cdot \mathbf{S}_j, \quad (68)$$

where we may set $H^x = 0$ without loss of generality (this can always be achieved by an appropriate rotation of the quanti-

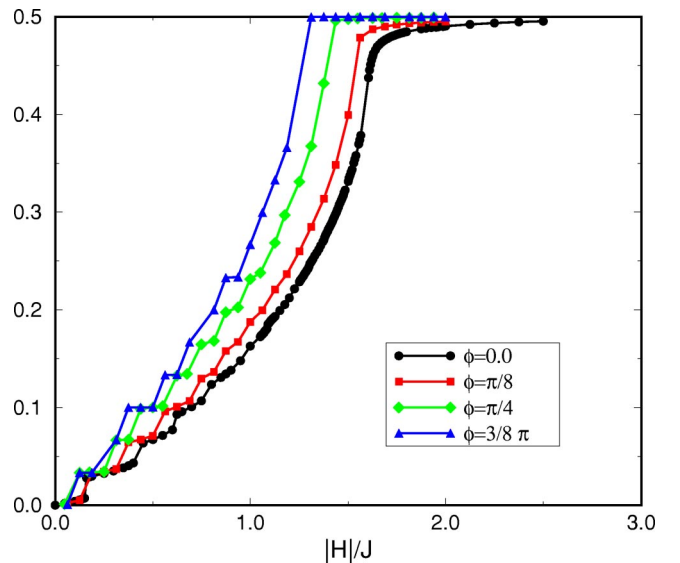


FIG. 16. DMRG results for the total magnetization for a magnetic field applied in the yz plane at various values of ϕ .

zation axis around the y direction). Rotating the spin quantization axis onto the direction of the field leads to the following Hamiltonian:

$$\mathcal{H} = J \sum_j \tilde{\mathcal{S}}_j \cdot \tilde{\mathcal{S}}_{j+1} + H \tilde{\mathcal{S}}_j^z + (\Delta - 1) \mathcal{H}'_{j,j+1}, \quad (69)$$

where $H = \text{sgn}(H^z) |\mathbf{H}|$ and

$$\begin{aligned} \mathcal{H}'_{j,j+1} = & \cos^2 \theta \tilde{\mathcal{S}}_j^y \tilde{\mathcal{S}}_{j+1}^y + \sin^2 \theta \tilde{\mathcal{S}}_j^z \tilde{\mathcal{S}}_{j+1}^z \\ & + \sin \theta \cos \theta [\tilde{\mathcal{S}}_j^z \tilde{\mathcal{S}}_{j+1}^z + \tilde{\mathcal{S}}_j^y \tilde{\mathcal{S}}_{j+1}^y]. \end{aligned} \quad (70)$$

Due to the presence of the $\tilde{\mathcal{S}}_j^y \tilde{\mathcal{S}}_{j+1}^z$ terms in Eq. (70) the resulting Hamiltonian can no longer be Jordan-Wigner transformed into an expression that is local in terms of Fermion operators. Hence the extension of the mean-field approximation to the case of an arbitrary orientation of the magnetic field is not straightforward.

We have investigated the effects of applying the magnetic field at an angle to the exchange anisotropy by means of DMRG computations of the magnetization. We parametrize the magnetic field by

$$\mathbf{H} = |\mathbf{H}| [\cos \phi \mathbf{e}^z + \sin \phi \mathbf{e}^y]. \quad (71)$$

We have determined $M = \sqrt{\langle S^z \rangle^2 + \langle S^y \rangle^2}$ and $M^z = \langle S^z \rangle$ by means of DMRG calculations for lattices of up to 50 sites for different values of ϕ . In Fig. 15 we show results for M^z and a field applied at an angle of $\phi = 45^\circ$. As expected we find that $M^z(\phi = 45^\circ) < M^z(\phi = 0)$, but in addition the kink in the magnetization curve occurs at a smaller value of $|H|/J$. In Fig. 16 we show the total ordered ferromagnetic moment M as a function of the magnitude of the applied field $|H|/J$ for several values of ϕ . The magnetization curve becomes steeper with increasing ϕ and approaches the magnetization curve for the XXZ chain in a longitudinal field for $\phi \rightarrow \pi/2$.

ACKNOWLEDGMENTS

We thank D.A. Tennant and especially R. Coldea for many important discussions and suggestions, and F. Capraro for providing us with his DMRG data. F.H.L.E. acknowledges important correspondence with A. Furusaki and T. Hikihara. Work at Brookhaven National Laboratory was carried out under Contract No. DE-AC02-98 CH10886, Division of Material Science, U.S. Department of Energy. J.-S.C. thanks the Institute for Strongly Correlated and Complex Systems at BNL for hospitality and support. U.L. thanks A. Kemper for valuable discussions.

-
- ¹D.A. Tennant, B. Lake, S.E. Nagler, and C.D. Frost (unpublished).
²M. Takahashi, Prog. Theor. Phys. **46**, 401 (1971); G. Müller, H. Thomas, H. Beck, and J.C. Bonner, Phys. Rev. B **24**, 1429 (1981); H.J. Schulz, *ibid.* **34**, 6372 (1986); A. Klümper, Z. Phys. **91**, 507 (1993); A.H. Bougourzi, M. Couture, and M. Kacir, Phys. Rev. B **54**, 12 669 (1996); N. Kitanine, J.-M. Maillet, N.A. Slavnov, and V. Terras, Nucl. Phys. B **641**, 487 (2002).
³J. Kurmann, H. Thomas, and G. Müller, Physica A **112**, 235 (1982).
⁴M. Kenzelmann, R. Coldea, D.A. Tennant, D. Visser, M. Hofmann, P. Smeibidl, and Z. Tylczynski, Phys. Rev. B **65**, 144432 (2002).
⁵D.V. Dmitriev, V.Y. Krivnov, and A.A. Ovchinnikov, Phys. Rev. B **65**, 172409 (2002); D.V. Dmitriev, V.Ya. Krivnov, A.A. Ovchinnikov, and A. Langari, JETP **95**, 538 (2002).
⁶Th. Niemeijer, Physica (Amsterdam) **36**, 377 (1967); **39**, 313 (1968).
⁷B.M. McCoy, E. Barouch, and D.B. Abraham, Phys. Rev. A **4**, 2331 (1971).
⁸J.D. Johnson and B.M. McCoy, Phys. Rev. A **4**, 2314 (1971).
⁹H.G. Vaidya and C.A. Tracy, Physica A **92**, 1 (1978).
¹⁰J.H. Taylor and G. Müller, Phys. Rev. B **28**, 1529 (1983).
¹¹F.H.L. Essler, Phys. Rev. B **59**, 14376 (1999).
¹²E. Barouch and B.M. McCoy, Phys. Rev. A **3**, 786 (1971).
¹³F. Capraro and C. Gros, cond-mat/0207279 (unpublished).
¹⁴K. Fabricius, U. Löw, and K.H. Mütter, Phys. Rev. B **44**, 9981 (1991).
¹⁵G. Müller and R.E. Shrock, Phys. Rev. B **32**, 5845 (1985).
¹⁶M. Oshikawa and I. Affleck, Phys. Rev. B **65**, 134410 (2002).
¹⁷S. Lukyanov, Nucl. Phys. B **522**, 533 (1998); S. Lukyanov, Phys. Rev. B **59**, 11 163 (1999).
¹⁸T. Hikihara and A. Furusaki, Phys. Rev. B **63**, 134438 (2001).
¹⁹T. Hikihara and A. Furusaki (unpublished).
²⁰F.H.L. Essler and A.M. Tsvelik, Phys. Rev. B **57**, 10 592 (1998).
²¹V.E. Korepin, A.G. Izergin, and N.M. Bogoliubov, *Quantum Inverse Scattering Method, Correlation Functions and Algebraic Bethe Ansatz* (Cambridge University Press, Cambridge, 1993).
²²I. Affleck and M. Oshikawa, Phys. Rev. B **60**, 1038 (1999).
²³S. Lukyanov and A. Zamolodchikov, Nucl. Phys. B **493**, 571 (1997).
²⁴C. Destri and H. de Vega, Nucl. Phys. B **358**, 251 (1991).
²⁵F. Smirnov, *Form Factors in Completely Integrable Models of Quantum Field Theory* (World Scientific, Singapore, 1992).
²⁶S. Lukyanov, Mod. Phys. Lett. A **12**, 2911 (1997).
²⁷S. Lukyanov and A. Zamolodchikov, Nucl. Phys. B **607**, 437 (2001).
²⁸A.A. Nersesyan, A. Luther, and F.V. Kusmartsev, Phys. Lett. A **176**, 363 (1993); A.O. Gogolin, A.A. Nersesyan, and A.M. Tsvelik, *Bosonization and Strongly Correlated Systems* (Cambridge University Press, Cambridge, 1998), Chap. 20.
²⁹V.M. Yakovenko, JETP Lett. **56**, 510 (1992).
³⁰S. Sachdev, *Quantum Phase Transitions* (Cambridge University Press, Cambridge, 1999).